

# Influence of La-Doping of $\text{YBa}_2\text{Cu}_3\text{O}_7$ on Transport Properties of Interface-Engineered Ramp-Edge Junctions

J.-K. Heinsohn, R. Dittmann, J. Rodríguez Contreras, J. Scherbel, A. Klushin, M. Siegel

**Abstract**— We have investigated the influence of La-doping of the  $\text{YBa}_{2-x}\text{La}_x\text{Cu}_3\text{O}_7$  (YBCO) thin film electrodes on dc and ac Josephson properties of ramp-edge junctions with interface-engineered barriers. Non-doped optimized junctions exhibit critical current densities,  $j_c$ , of  $5 \cdot 10^4 \text{ A/cm}^2$  and normal sheet resistances,  $R_N A$ , of  $3 \cdot 10^{-9} \text{ Ohm} \cdot \text{cm}^2$  at 77 K. The transport properties of junctions with  $x = 0.03$  La-doping are quite similar to those of non-doped junctions. La-doping of  $x = 0.05$  and  $x = 0.07$  leads to an increase of  $R_N A$  and decrease of  $j_c$  by about one order of magnitude. Devices with  $j_c < 10^4 \text{ A/cm}^2$ , which are operating in the short junction limit exhibit current-voltage characteristics without any excess current and 100 % modulation of critical current in external magnetic field. The current voltage characteristics exhibit well defined Shapiro steps. The dependence of current-step height on microwave current can be described in the resistively-shunted junction model. The strong changes in the temperature dependencies of  $j_c$  and  $R_N A$  suggest different electrical transport properties for junctions fabricated with non-doped and La-doped YBCO. The temperature dependence of the critical current and the normal resistance allows us to draw conclusions to the transport properties of our junctions.

**Index Terms**— Josephson junctions, interface engineering

## I. INTRODUCTION

INTERFACE-Engineered junctions (IEJ) are an interesting approach for the realization of reliable and controllable High-Temperature Superconductor (HTS) Josephson junctions. For most applications in superconducting electronics, e.g. SQUID, digital circuits or voltage calibrators, RCSJ-like junctions (Resistively-Capacitively-Shunted Junction model) are required. Nevertheless, no detailed comparison of the static and dynamic properties of IEJ's to the RCSJ-model at different temperatures have been published up to now. Several groups are employing IEJ's by using different approaches for the interface treatment [1 – 6]. All approaches use an ion treatment of the ramp and a subsequent annealing step, but the methods and the process parameters differ strongly from group to group. The published current densities, the normal resistances and the suggested transport mechanisms differ for the junctions fabricated in different ways. Some groups observe properties

of an insulating barrier containing localized states [4, 5] whereas previous results of our group report on a metallic behavior of the barrier material [6].

The presence of La either in the superconducting electrodes or in the insulator influences the properties of the junctions. Hunt et al. observed a strong increase of the normal resistance and a decrease of the critical current [2]. Satoh et al. observed RCSJ-like current-voltage characteristics (IVC) only if La is present in the ramp area [5].

We will present detailed measurements of the transport properties of interface-engineered junctions with YBCO (non-doped junctions) as well as with  $\text{YBa}_{1.95}\text{La}_{0.05}\text{Cu}_3\text{O}_7$  electrodes (La(5%)-doped junctions). We will compare the properties of the junctions with and without doping. The properties will be discussed in terms of the RCSJ model.

## II. Junction preparation

First, a bi-layer consisting of a 120 nm thick  $\text{YBa}_{1.95}\text{La}_{0.05}\text{Cu}_3\text{O}_7$  film and a 220 nm thick  $\text{SrTiO}_3$  (STO) film are deposited in-situ by pulsed laser deposition. We employed STO as well as  $\text{LaAlO}_3$  as substrate materials and did not observe any influence on the film quality or junction properties. The YBCO films are deposited at a substrate temperature of  $T = 805^\circ\text{C}$ , oxygen pressure  $p = 60 \text{ Pa}$ , energy density of  $2 \text{ J/cm}^2$ , and a laser frequency of 10 Hz. The STO films deposited in situ on top of the YBCO films are fabricated at  $T = 760^\circ\text{C}$ ,  $p = 15 \text{ Pa}$ , with the same energy density and frequency as for YBCO. Further details can be extracted from [8]. For the fabrication of the ramps, the bilayers are patterned by conventional photolithography and ion-beam etching in a Kaufmann-type source using an current density of  $0.25 \text{ mA/cm}^2$  and an energy of 250 eV. A detailed description of the ramp fabrication process can be found in [8]. The process results in ramps with edge angles of  $20^\circ$  for STO and  $30^\circ$  for YBCO. The interface engineering consists of a short milling step at higher voltages and an annealing step in the deposition chamber. We investigated the parameters for these steps in combination with the deposition temperature of the counter electrode by statistical methods [8]. For optimal barrier treatment, we use a 5 min treatment at an acceleration voltage of 1200 V and a 30 min annealing step at  $500^\circ\text{C}$  at the deposition pressure of 60 Pa in the vacuum chamber. The counter electrode is deposited at  $760^\circ\text{C}$ . The junctions are patterned by conventional photolithography and Ar-ion-

Manuscript received September 18, 2000. This work was supported in part by the German DFG Project N° Si 704/1-1.

The authors are with the Forschungszentrum Jülich GmbH, Institut Schicht- und Ionentechnik, 52425 Jülich, Germany (telephone: +49-2461-613793, e-mail: m.siegel@fz-juelich.de).

beam milling. Finally, a 200 nm thick gold layer is evaporated and patterned by a lift-off process to provide electrical contacts.

### III. TRANSPORT PROPERTIES

The Josephson junctions are measured in the standard four-point technique and are shielded against external magnetic fields by a Cryoperm shield. All of our interface-engineered junctions are very sensitive to flux trapping which leads to a suppression of the maximal critical current at zero magnetic field. We applied a small external magnetic field to adjust the critical current to the maximal value to compensate the effect of trapped flux. The normal resistance,  $R_N$ , is determined by the slope of the linear part of the I-V curves at high bias currents.

#### A. Influence of La-doping

Fig. 1 shows the IVC measured from a 3  $\mu\text{m}$  wide junction with 5% La content. The form of the IVC behaves close to the RCSJ-model. The current density of the junction, shown in Fig. 1, is  $j_c = 4.2 \cdot 10^4 \text{ A/cm}^2$  and the sheet resistance  $R_N A = 4.2 \cdot 10^{-9} \Omega \cdot \text{cm}^2$ . The critical current density of the La(5%)-doped junctions is about one order of magnitude lower and the normal sheet resistance is about one order of magnitude higher than for non-doped junctions. Similar results have been observed by other groups [2]. Since a high concentration of La reduces the critical temperature,  $T_c$ , of YBCO, one possible explanation for the difference between non-doped junctions and La(5%)-doped junctions could be that La diffuses in the ramp area and an agglomeration of La results in an interface layer with reduced  $T_c$  forming an additional barrier. In terms of the assumption, it seems possible to adjust the parameters of the junction by the La content. Therefore, we investigated junctions fabricated with electrodes of doping levels from 0%-7%. We observed 2 groups of junctions. For La(5%)-doped junctions and La(7%)-doped junctions, the critical current is about one order of magnitude lower and the normal resistance is about one order of magnitude higher than for the La(3%)-doped junctions and La(0%)-doped junctions. That means that a threshold of La content is needed to change the junction parameters, but it is impossible to continuously adjust the parameters of the junction. Due to these results, it seems unlikely that the La content itself determines the electrical properties of the barrier. However, La is prerequisite for the formation of the barrier layer. To further investigate the role of La in the preparation process, we fabricated junctions where  $\text{YBa}_{1.95}\text{La}_{0.05}\text{Cu}_3\text{O}_7$  (La(5%)-doped YBCO) was used either only for the base electrode or only for the counter electrode. The junctions with La(5%)-doped YBCO bottom electrodes behave like junctions where both electrodes consist of La(5%)-doped YBCO. The junctions with the La(5%)-doped YBCO top electrodes behave like non-doped junctions. This shows that no simple interdiffusion of La takes place which could as well occur during the fabrication of the counter electrode. We found that La has to be present during etching and annealing to influence the formation of

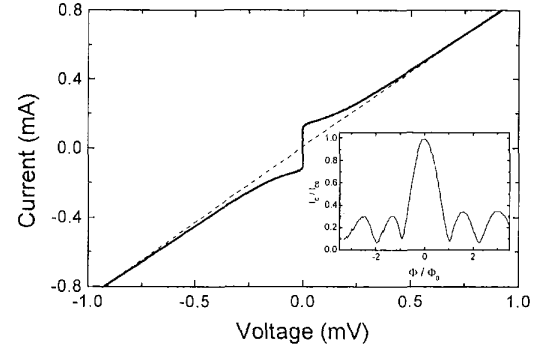


Fig. 1. I-V curve of a 3  $\mu\text{m}$  wide La(5%)-doped junctions at 77 K. The inset shows the modulation of the critical current with magnetic flux.

the barrier. Hunt et al. [2] suggested that during the treatment of the ramp, the La atoms interchange in the interface region with a much higher probability with Y than Ba atoms do. On the other hand, Wen et al. observed by TEM that in case they utilize the La-containing insulator  $(\text{La}_{0.3}\text{Sr}_{0.7})(\text{Al}_{0.65}\text{Ta}_{0.35})\text{O}_3$  the barrier is continuous whereas for  $\text{SrTiO}_3$  a high number density of pin holes is observed [7]. We performed TEM investigations of our junctions but no barrier layer could be detected neither for the La(0%)-doped junctions nor for the La(5%)-doped junctions.

The inset of Fig. 1 shows the  $I_c(H)$  dependence of a 3  $\mu\text{m}$  La(5%)-doped junction at 65 K. The  $I_c(H)$ -pattern is very similar to the Fraunhofer pattern. The IVC can be well described by the RCSJ-model and no significant amount of excess current is observed. A detailed investigation of the  $I_c(H)$ -patterns of our junctions will be published elsewhere [9].

For lower temperatures, deviations of the IVC from the RSJ-model and from the Fraunhofer-pattern become significant. This behavior can be explained by self-field effects because with decreasing temperatures the current density increases leading to an increasing Josephson penetration depth,  $\lambda_J = \sqrt{\hbar/2e\mu_0 d' j_c}$  with  $d' = d + 2\lambda_L$ . At 65 K, the critical current density is  $j_c = 8.5 \cdot 10^3 \text{ A/cm}^2$  corresponding to  $w/\lambda_J = 1.4$ , where  $w$  is the width of the junction. While at 45 K, the critical current density is  $j_c = 1.1 \cdot 10^5 \text{ A/cm}^2$  which corresponds to  $w/\lambda_J = 5$ . Therefore the behavior of the junctions changes from the short to the long junction regime. La(5%)-doped junctions are in the short junction limit in the whole temperature range, but start to have a significant amount of excess current at 50 K.

In the case of the non-doped junctions, the IVC show ideal RSJ-behavior only in the vicinity of  $T_c$ . Below 55 K, the IVC are already flux-flow like because of the high current density. Therefore, non-doped junctions are not suitable for applications which require RSJ-behavior below 77 K.

#### B. Influence of Microwave Irradiation

We investigated the dynamic properties of La(5%)-doped junctions in more detail. Fig. 2 shows the IVC of a 3  $\mu\text{m}$

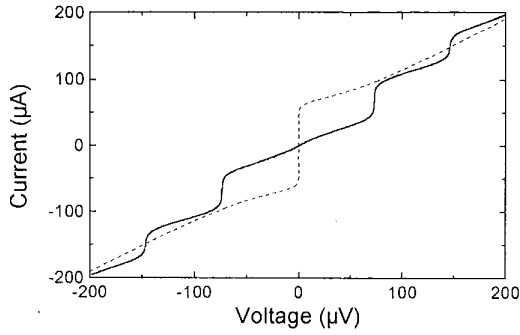


Fig. 2. IVC of a 3  $\mu\text{m}$  wide La(5%)-doped junction at 55 K. The dotted line shows the IVC without microwave irradiation. The continuous lines corresponds to the IVC under 28.8 GHz irradiation.

wide junction with and without microwave irradiation at 55 K. With  $w/\lambda_J=2.8$ , the junction is clearly in the short junction regime and no significant excess current is visible. The parameters of the junctions are  $I_C = 260 \mu\text{A}$ ,  $R_N = 1 \Omega$  leading to a characteristic voltage of  $I_C R_N = 260 \mu\text{V}$ . Fig. 3 shows the experimental and simulated dependence of the heights of the 0<sup>th</sup>, 1<sup>st</sup> and 2<sup>nd</sup> Shapiro steps on the microwave current at 55 K. We have simulated the dependence of the heights of Shapiro steps on microwave current within the RCSJ-model [13] by solving the differential equation for the

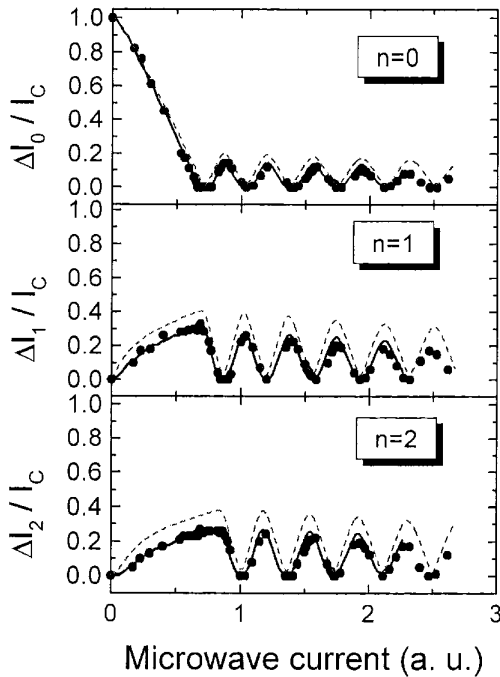


Fig. 3 Dependence of the 0<sup>th</sup>, 1<sup>st</sup> and 2<sup>nd</sup> Shapiro step heights of the junction shown in Fig. 2 on microwave current at 55 K and 28.8 GHz (circles). The dotted lines show the simulation without noise for  $\Omega = 0.23$  and  $\beta_c = 0.1$ ; the continuous lines show the simulation with noise for  $\Gamma = 0.016$ .

phase difference numerically [14, 15]. To obtain the fit shown in Fig. 3, we adjusted the critical current to the experimental value, and scaled the microwave current amplitude to the first minimum of the  $n=0$  step. The reduced frequency  $\Omega = \Phi_0 f_{\text{ext}} / (I_C R_N)$  is chosen to approximate the periodicity of the experimental step height with microwave current. Here  $f_{\text{ext}}$  is the external frequency of microwave irradiation,  $I_C$  and  $R_N$  are critical current and normal resistance, respectively and  $\Phi_0 = h/2e$ . The simulation gives optimal results (see Fig. 3) for the parameters  $\Omega=0.23$ ,  $\beta_c=0.1$  and  $\Gamma=0.016$ . The parameter  $\Gamma$  describes the thermal noise energy in the junction and is  $\Gamma = 2k_B T / (\Phi_0 I_C)$ , where  $k_B$  is the Boltzmann constant. The Steward-McCumber parameter  $\beta_c$  is given by  $\beta_c = 2e I_C R_N^2 C / \hbar$ . Fig. 3 shows also the result of simulation without additional thermal noise. Though some amount of excess current is present at 55 K the dynamic properties can be well described by the RCSJ-model. For  $w/\lambda_J > 4$  we observe sub-harmonic steps in the I-V characteristics of this junction as predicted for Josephson junctions in the long junction regime

#### IV. CURRENT TRANSPORT PROPERTIES

The resistance of the non-doped junction decreases with decreasing temperature to about 40 K as could be expected for a metallic barrier. Below 40 K, the resistance is temperature independent. A possible explanation is the existence of a superconducting layer with a reduced  $T_C$  ( $S'$ ) at the interface between the base electrode and counter electrode. The critical temperature could be about 40 K where the metallic temperature dependence of  $R_N$  renders temperature independent. The residual resistance could be due to the dissipation of fluxons in the superconducting microbridge. Another explanation is a combination of a temperature independent boundary resistance and a normal conducting N- or  $S'$ -layer. It is difficult to distinguish between a N-layer and a  $S'$ -layer if an additional interface layer with a finite resistance is present. It is more likely to attribute the metallic properties to an  $S'$ -layer because YBCO becomes a disordered hopping insulator as soon as  $T_C$  is completely suppressed by the presence of defects. The resistance of a La(5%)-doped junction decreases with decreasing temperature in the temperature range above 50 K. Below 50 K, there is a striking difference to the non-doped junctions, since  $R_N$  increases with decreasing temperature.

The analysis of the temperature dependence of  $R_N$  at temperatures below 50 K revealed that the temperature-dependent contribution to the conductivity has a behavior which correlates with of the Glazman-Matveev theory [10] of resonant tunneling via one and two localized states.

However, the temperature dependence of  $R_N$  below 50 K shows that there exists an insulating layer with a high number density of localized states at the interface which determines the quasiparticle transport at low temperatures. Above 50 K, the conductivity is so high that  $R_N$  is dominated by the metallic-like layer. Therefore we suggest that the interface consists of a  $S'$ -layer which is covered by a thin

insulating layer. Since we did not observe a different material at the interface by TEM, the layers with the different electrical properties have to be identified with orthorhombic YBCO with different levels of damage. The fact that the properties of our junctions are stable in time and against oxygen annealing treatments suggests cation disorder as origin of the  $T_C$  suppression in the S'-layer instead of defects in the oxygen sub-lattice.

For the quasiparticles, metallic as well as resonant tunneling transport channels exist in our interface engineered junctions. In the case of the non-doped junctions, where mainly metallic quasiparticle transport is observed, one could expect the proximity effect to be responsible for the Cooper-pair exchange between the superconducting electrodes. Superconductor-Normal metal-Superconductor (SNS) models should be suitable to describe the properties of our junctions. Our estimations show that even in the case of the La(0%)-doped junctions, the barrier layer does not consist of a single N- or S'-layer. Especially, the linearity in the whole temperature regime rules out the existence of a single S'-layer at the interface, because the critical current should increase drastically below  $T_C$  of the S'-layer. A quasi-linear temperature dependence was observed for most HTS junctions [11] and can be explained taking into account local inhomogeneities of the barrier or the interface. For example, an Superconductor-constriction-Superconductor (ScS) model was used to fit the  $I_C(T)$  dependence of HTS junctions with Au interlayer [12]. In our case, it is reasonable to regard a ScNS model. In more detail, these results will be discussed and simulated elsewhere.

#### V. SUMMARY

Interface-engineered junctions have been fabricated by using  $\text{YBa}_2\text{Cu}_3\text{O}_7$  as well as  $\text{YBa}_{2-x}\text{La}_x\text{Cu}_3\text{O}_7$  for the superconducting electrodes and the role of La-doping in our fabrication process has been investigated. Non-doped optimized junctions exhibit critical current densities,  $j_C$ , of  $5 \cdot 10^4 \text{ A/cm}^2$  and normal sheet resistances,  $R_N A$ , of  $3 \cdot 10^{-9} \text{ Ohm} \cdot \text{cm}^2$  at 77 K. The critical current density of the La(5%)-doped junctions is about one order of magnitude lower than the critical current density of the non-doped junctions while the normal sheet resistance is about one order of magnitude higher. We found that the properties of the junctions can not be continuously adjusted by the La content but there exists a threshold value of about 5% for La to influence the junction properties. This shows that La is prerequisite for the formation of the barrier but does not form the barrier by local doping of the interface.

At current densities where the junctions are in the short junction regime ( $w/\lambda_J < 4$ ), the static IVC as well as the IVC under microwave irradiation can be well described by the RCSJ-model. The  $I_C(H)$ -pattern in this regime is very similar to a Fraunhofer-pattern. Junctions with  $w/\lambda_J > 4$  showed deviations from the RCSJ-model. In the case of the non-doped junctions, the current densities are so high that ideal RCSJ-behavior can be observed only near  $T_C$ . The La(5%)-

doped junctions are short junctions above 50 K and therefore they are more suitable for applications in superconducting electronics.

We propose a model of a barrier consisting of a layer with reduced  $T_C$  which is covered by an insulating layer containing microshorts (constrictions) and localized states. We suggest these layers to be YBCO with different degrees of cation disorder induced by the ion milling treatment. The presence of La reduces the number density and the diameter of the constrictions. As a result, the quasiparticle current transport in the La(5%)-doped junctions occurs by resonant tunneling via localized states in the insulating layer.

#### ACKNOWLEDGMENT

The authors thank C.L. Jia for high resolution TEM analysis and R. Debusmann for technical support in the laser ablation process.

#### REFERENCES

- [1] B. H. Moeckly and K. Char, "Properties of interface-engineered high  $T_C$  Josephson junctions", *Appl. Phys. Lett.* vol. 71, pp. 2526-2529, 1997.
- [2] B. D. Hunt, M. G. Forrester, J. Talvacchio, and R. M. Young, "High-Resistance HTS Edge Junctions for Digital Circuits", *IEEE Trans. Appl. Supercond.*, vol. 9 pp. 3362-3365, 1999.
- [3] Y. Soutome, T. Fukazawa, A. Tsukamoto, Y. Tarutani, and K. Takagi, "Study on the optimization of ramp-edge surface for  $\text{YBa}_2\text{Cu}_3\text{O}_{7-x}$  ramp-type Josephson junctions", *International Workshop on Superconductivity, Extended Abstracts*, pp. 113-116, 1999.
- [4] A. Fujimaki, K. Kawai, N. Hayashi, M. Horibe, M. Maruyama, and H. Hayakawa, "Preparation of Ramp-Edge Josephson Junctions with Natural Barriers", *IEEE Trans. Appl. Supercond.* vol. 9, pp. 3436-3439, 1999.
- [5] T. Satoh, M. Hidaka, and S. Tahara, "High-Temperature Superconducting Edge-Type Josephson Junctions with Modified Interfaces", *IEEE Trans. Appl. Supercond.* vol. 9, pp. 3141-3144, 1999.
- [6] R. Dittmann, J.-K. Heinsohn, A.I. Braginski, and C.L. Jia, "Fabrication of  $\text{YBa}_2\text{Cu}_3\text{O}_7$  Ramp-Type Junctions by Interface Treatments", *IEEE Trans. Appl. Supercond.*, vol. 9, pp. 3440-3443, 1999.
- [7] J.G. Wen, N. Koshizuka, S. Tanaka, T. Satoh, M. Hidaka, and S. Tahara, "Atomic Structure and Composition of the Barrier in the Modified Interface High- $T_C$  Josephson Junction Studied by Transmission Electron Microscopy", *Appl. Phys. Lett.*, vol. 75, pp. 2470-2472, 1999.
- [8] J.-K. Heinsohn, R.H. Hadfield, and R. Dittmann, "Effects of process parameters on the fabrication of edge-type YBCO Josephson junctions by interface treatments", *Physica C*, vol. 326-327, pp. 157-161, 1999.
- [9] J.-K. Heinsohn, R. Dittmann, J. Rodríguez Contreras, A. Klushin, E. Goldobin, M. Siegel, R. Pöpel, D. Hagendorn, F.M. Buchholz, to be submitted to *Physica C*.
- [10] L.I. Glazman and K.A. Matveev, "Inelastic tunneling across thin amorphous films", *Sov. Phys. JETP*, vol. 67, pp. 1276-1213, 1988.
- [11] K. A. Delin and A. W. Kleinsasser, "Stationary properties of high-critical-temperature proximity effect Josephson junctions", *Supercond. Sci. Technol.*, vol. 9, pp. 227-269, 1996.
- [12] M. Bode, M. Grove, M. Siegel, and A. I. Braginski, "Superconductor-normal-superconductor step-edge junctions with Au barriers", *J. Appl. Phys.*, vol. 80, pp. 6378-81, 1996.
- [13] W.C. Steward, "Current voltage characteristics of Josephson junctions", *Appl. Phys. Lett.*, vol. 12, pp. 277-280, 1968; D.E. McCumber, "Effect of ac impedance on dc voltage-current characteristics of superconductor weak-link junctions", *J. Appl. Phys.* vol. 39, pp. 3113-3117, 1968.
- [14] P. Russer, "Influence of microwave radiation on current-voltage characteristic of superconducting weak links", *J. Appl. Phys.*, vol. 43, pp. 2008-2010, 1972.
- [15] M. Siegel, E. Heinz, P. Seidel, V. Hilarius, "Josephson effect on YBCO break junctions", *Z. Phys. B*, vol. 83, pp. 323-326, 1991.